NJC

ROYAL SOCIETY OF CHEMISTRY

PAPER

View Article Online
View Journal | View Issue



Cite this: *New J. Chem.*, 2025, 49, 3877



# Can we predict specific numbers of catalytically important molecules of water in H/D exchange in aromatic systems? A combined NMR and DFT study†

Photini Chalkidou, Themistoklis Venianakis, George Papamokos, Michael Siskos* and Ioannis P. Gerothanassis*

Base-catalyzed H/D exchange reactions through keto–enol tautomeric equilibrium are a textbook example in mechanistic organic chemistry. The pH effect of $H_2O$ catalysis, however, is largely unknown. We report, herein, variable temperature and pD $^1$H NMR studies of the experimental activation enthalpy $\left(\Delta H^{\ddagger}_{exp}\right)$, entropy $\left(-T\Delta S^{\ddagger}_{exp}\right)$, and Gibbs free energy $\left(\Delta G^{\ddagger}_{exp}\right)$ of H/D exchange reactions of the H-6 and H-8 protons belonging to ring A of the natural product taxifolin. The experimental $\Delta G^{\ddagger}_{exp}$ values range from ~25 to 23 kcal mol$^{-1}$ for pD values of 6.1 to 9.6 and a buffer concentration in the range of 25 to 1000 mM. Differences in $\Delta G^{\ddagger}_{exp}$ values of neutral and anionic taxifolin and phloroglucinol were found to be very small ($\lesssim$1.5 kcal mol$^{-1}$). The experimental data of taxifolin and phloroglucinol were compared with DFT calculations with two up to four $H_2O$ molecules explicitly present, which demonstrate a unique catalytic role of $H_2O$ of over 35 kcal mol$^{-1}$. Excellent agreement between $\Delta G^{\ddagger}_{exp}$ and DFT calculated Gibbs free activation energies, $\Delta G^{\ddagger}_{comp}$, was obtained with the use of three molecules of $H_2O$ for the neutral state of phloroglucinol (with the "in–in" configuration of the phenol OH groups) and taxifolin. In the ionic form of phloroglucinol, the mechanistic pathway with two molecules of $H_2O$ in the transition state (one of which involves the C=O moiety) showed very good agreement with the experimental data. For the anionic form of taxifolin, the mechanistic pathway with three molecules of $H_2O$ in the transition state showed excellent agreement with the experimental $\Delta G^{\ddagger}_{exp}$ values. Among the various functionals used, the APFD/6-31+G(d) and B3LYP/6-31+G(d)/GD3BJ resulted in optimum agreement with $\Delta G^{\ddagger}_{exp}$. The enthalpic term $\Delta H^{\ddagger}_{comp}$ is considerably larger than the entropic term $\Delta S^{\ddagger}_{comp}$, in agreement with the experimental data. This indicates a dissociative mechanism of the loosely bound activated complex. The present results demonstrate the unique catalytic role of two and/or three molecules of $H_2O$, through keto–enol tautomerization, with minor contribution of base-catalysis, in H/D exchange reactions in aromatic systems.

Received 22nd July 2024,
Accepted 3rd February 2025

DOI: 10.1039/d4nj03276d

rsc.li/njc

## 1. Introduction

The significant role of $H_2O$ in enhancing the rate/selectivity in the aqueous phase or adsorbed $H_2O$ molecular environment has been extensively emphasized and reviewed in recent literature.[1–5] The cooperative hydrogen bond network formed by $H_2O$ molecules can significantly affect the structural and electronic properties of solute molecules. Thus, $H_2O$ solvation can result in ionic dissociation and classical acid–base catalysis of organic reactions as a proton donor or an acceptor reaction partner. However, addressing how discrete solvation molecules of $H_2O$ affect chemical reactivity at the atomic level is a complex issue requiring an appropriate combination of experimental and computational methods.[1–6]

Acid- and base-catalyzed H/D exchange in aromatic systems is a textbook example in mechanistic organic chemistry. Thus, acid-catalyzed H/D electrophilic aromatic substitution reactions have been extensively utilized since the 1960s with the use of strong deuterated Brønsted or Lewis acids[7–11] in the formation of a non-classical σ-carbocation. Base-catalyzed H/D exchange reactions

*Section of Organic Chemistry and Biochemistry, Department of Chemistry, University of Ioannina, Ioannina, GR, 45110, Greece. E-mail: msiskos@uoi.gr, igeroth@uoi.gr*

† Electronic supplementary information (ESI) available: Tables of computational data. See DOI: https://doi.org/10.1039/d4nj03276d

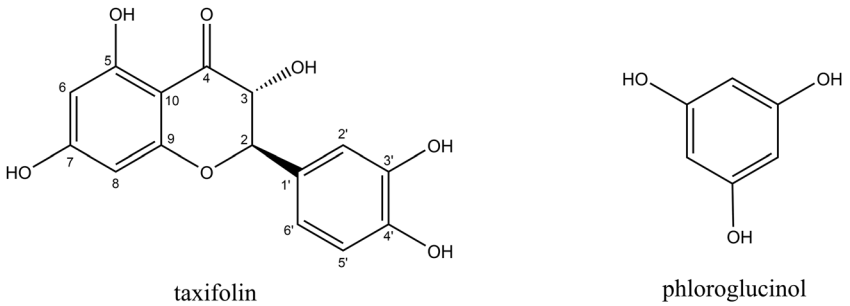


Scheme 1 Structures of taxifolin and phloroglucinol.

can also provide an alternative method, which has been extensively utilized since the 1960s for the exchange of aromatic protons through keto–enol equilibrium.[10,12–14] To the best of our knowledge, the first report demonstrating the catalytic role of $H_2O$ appeared in 2015 by Mehr *et al.*[15] in the deuteration of aromatic rings through keto-enamine tautomeric equilibrium. The computational activation energy was found to be significantly reduced with the incorporation of a chain of five $H_2O$ molecules. Bonaldo *et al.*[16] reported $^1$H NMR kinetic measurements of the H/D exchange process on ring A of several classes of flavonoids. It was suggested that the reaction mechanism involves a slow, solvent-mediated, C–D bond formation/O–D bond breaking followed by a fast solvent-mediated C–H bond breaking/O–D bond formation resulting in the aromaticity of ring A. DFT calculations with a single solvation molecule of $H_2O$ resulted in a significant reduction in the activation energy which, however, was found to be ~30 kJ mol$^{-1}$ higher than the experimental values. Fayaz *et al.*[17] reported the direct activation of aromatic C–H bonds in polyphenolic compounds in a single step, using $D_2O$, at neutral pD and near ambient temperatures. NMR and DFT calculations supported the significant catalytic role of two $H_2O$ molecules in a keto–enol tautomerization process.

From the above, it is evident that: (i) $H_2O$ molecules can have a very significant role in the transition states and activation energy barriers and also in the selection of a reaction pathway through $H_2O$-mediated hydrogen/deuterium reaction mechanisms,[1–6,16–26] and (ii) the traditional and widespread rational behind the primary role of acid or basic catalysis of H/D exchange in aromatic systems is incomplete. Along these lines, we report herein detailed variable temperature and pD dependent $^1$H NMR and DFT computational studies of neutral and ionic states of taxifolin and phloroglucinol (Scheme 1) in

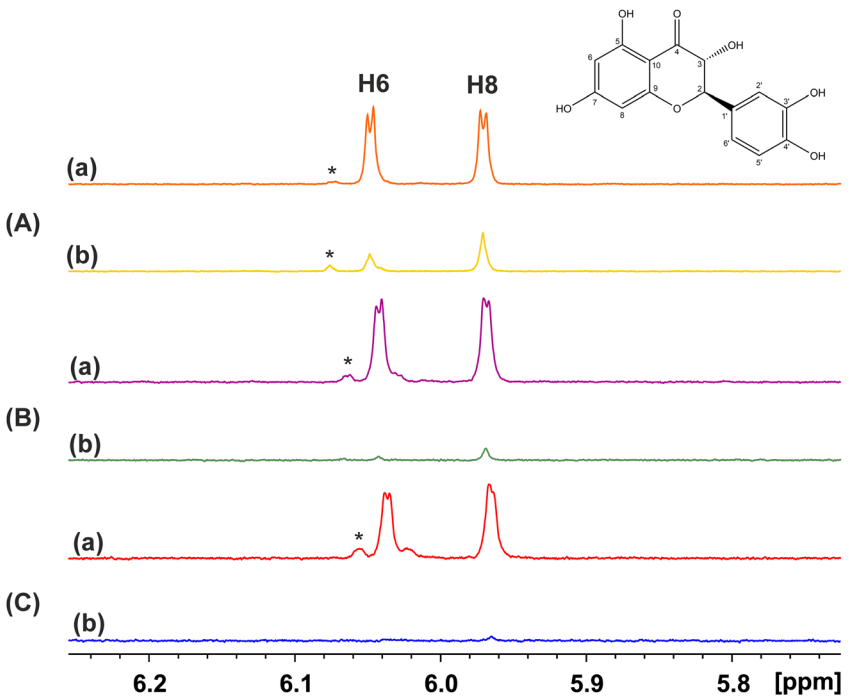


Fig. 1 1D $^1$H NMR (500 MHz) spectral region illustrating H-6 and H-8 H/D exchange of taxifolin (2.5 mM) in $D_2O$, phosphate buffer (25 mM), pD = 6.00. The spectra A(a) ($T$ = 313 K), B(a) ($T$ = 323 K), and C(a) ($T$ = 328 K) were recorded at a time interval of 0 h. The spectra A(b) ($T$ = 313 K), B(b) ($T$ = 323 K), and C(b) ($T$ = 328 K) were recorded at a time interval of 14 h.

 

an effort to investigate whether specific numbers of $H_2O$ molecules[6,27,28] can play a significant catalytic role in the H/D exchange process in polyphenolic aromatic systems.

## 2. Results and discussion

### 2.1. NMR studies

The H/D exchange reaction of taxifolin was investigated using 1D $^1$H NMR spectroscopy with variable temperatures, pD and concentrations of phosphate buffer. The assignment of the resonances was confirmed using 2D $^1$H–$^{13}$C HSQC and HMBC experiments. Fig. 1 illustrates $^1$H NMR spectra of the H-6 and H-8 protons of taxifolin recorded at pD = 6.00 and various temperatures and time intervals. The aromatic protons of the ring B do not undergo H/D exchange and, thus, were used as an integration reference along with the reference compound TSP-$d_4$. The H/D exchange at C-8 and C-6 protons of ring A, in contrast, was clearly observed at pD = 6.0, 7.6 and 9.6 and at various temperatures and buffer concentrations. The decay of the NMR signals of the C-6 and C-8 protons as a function of time was recorded at pD values 6.0 (Fig. 2 and 3) and 9.6

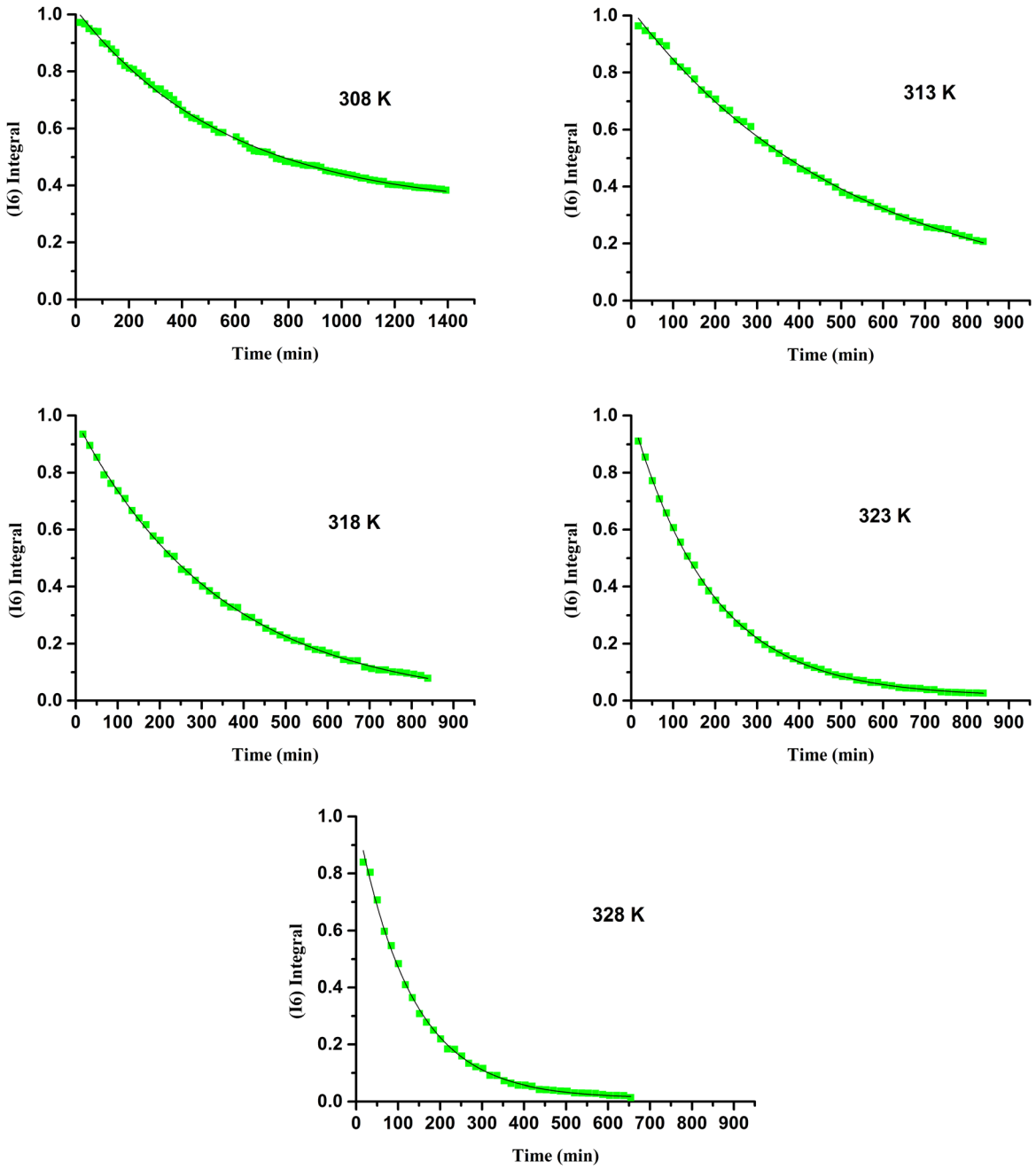


Fig. 2 H-6 H/D exchange kinetic curves of taxifolin (2.5 mM) in $D_2O$, phosphate buffer (25 mM), and pD = 6.00 at various temperatures.

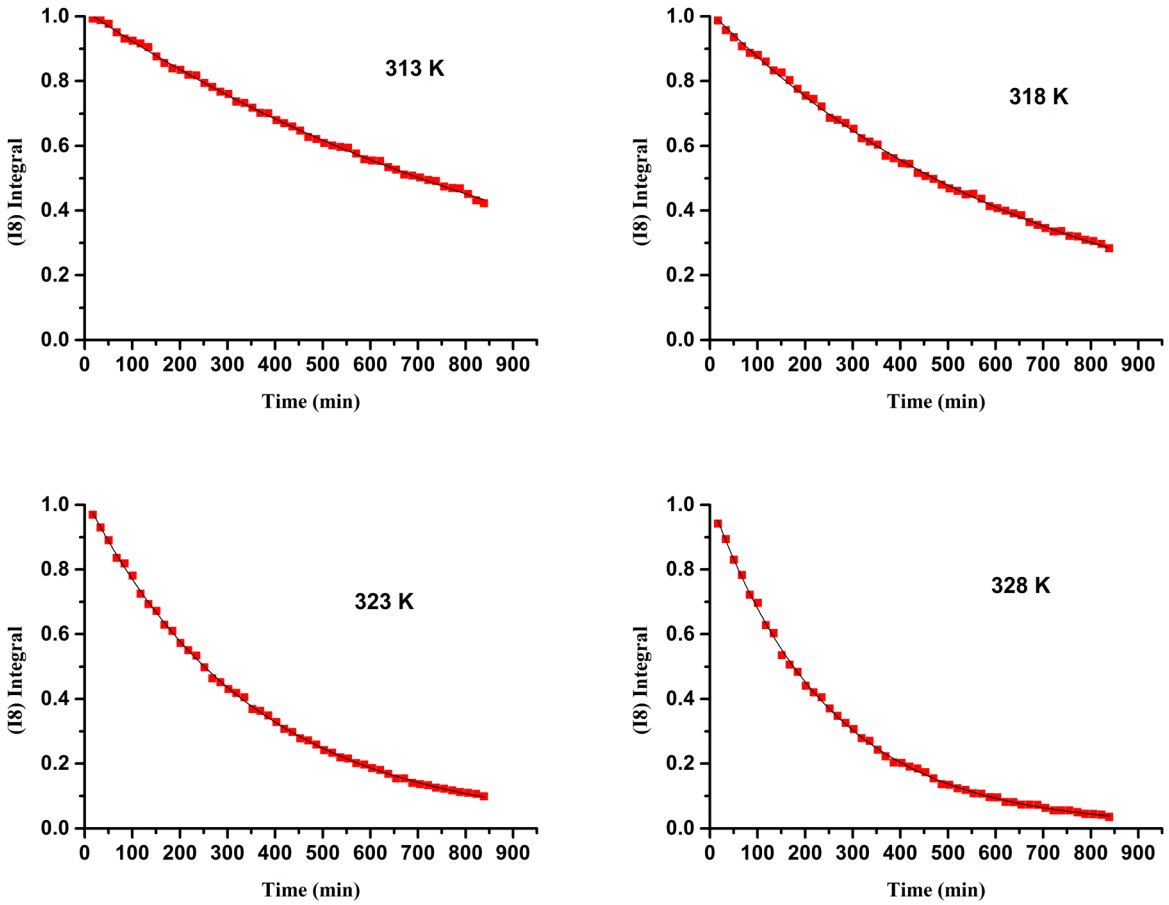


Fig. 3 H-8 H/D exchange kinetic curves of taxifolin (2.5 mM) in $D_2O$, phosphate buffer (25 mM), and pD = 6.00 at various temperatures.

(Fig. 4 and 5). At pD = 6.0 taxifolin exists essentially in the neutral form and at pD = 9.6 in the mono-deprotonated form.[29] The relative integrals of the C-8 and C-6 protons follow first-order kinetics with reactivity order C-6 > C-8 protons, with an increase in the exchange rate at pD = 9.60 as compared with pD = 6.00.

The Gibbs energy of activation, $\Delta G^{\ddagger}_{exp}$ (kcal mol$^{-1}$), is given by:

$$\Delta G^{\ddagger}_{exp} = \Delta H^{\ddagger}_{exp} - T\Delta S^{\ddagger}_{exp} \quad (1)$$

where $\Delta H^{\ddagger}_{exp}$ is the enthalpy of activation (kcal mol$^{-1}$) and $\Delta S^{\ddagger}_{exp}$ is the entropy of activation (kcal mol$^{-1}$ K$^{-1}$). According to the Eyring equation:

$$\ln\frac{K}{T} = -\frac{\Delta H^{\ddagger}_{exp}}{R}\frac{1}{T} + \ln\frac{k_B}{h} + \frac{\Delta S^{\ddagger}_{exp}}{R} \quad (2)$$

where $k_B$ is the Boltzmann's constant, $T$ is the absolute temperature in Kelvin ($K$), $K$ is the rate constant in s$^{-1}$, $R$ is the ideal gas constant, and $h$ is the Planck's constant. The values for $\Delta H^{\ddagger}_{exp}$ and $\Delta S^{\ddagger}_{exp}$, therefore, can be determined from kinetic data, obtained from a $\ln\frac{K}{T}$ *vs.* $\frac{1}{T}$ plot, with a negative slope, $-\frac{\Delta H^{\ddagger}_{exp}}{R}$, and a $y$-intercept $\frac{\Delta S^{\ddagger}_{exp}}{R} + \ln\frac{k_B}{h}$. Fig. 6 shows Eyring plots of the H-6 and H-8 protons of taxifolin (2.5 mM) in $D_2O$, phosphate buffer 25 mM and at pD = 6.00 with very good linear regression correlation coefficients ($R^2$ = 0.988 for H-6 and 0.982 for H-8).

The resulting $\Delta H^{\ddagger}_{exp}$, $-T\Delta S^{\ddagger}_{exp}$ and $\Delta G^{\ddagger}_{exp}$, for H/D exchange of taxifolin for various pD and phosphate buffer concentrations, are shown in Table 1. In all cases, the enthalpy term $\Delta H^{\ddagger}_{exp}$ makes a major contribution to $\Delta G^{\ddagger}_{exp}$ values with a minor entropic $\Delta S^{\ddagger}_{exp}$ term contribution. The $\Delta G^{\ddagger}_{exp}$ values for H-8 and H-6 protons were found to be in the range of 24.67 to 25.01 and 22.81 to 24.53 kcal mol$^{-1}$, respectively. The effect of phosphate buffer concentration (25 mM to 1 M) on $\Delta G^{\ddagger}_{exp}$ values was $\leq$ 0.7 kcal mol$^{-1}$, thus, its catalytic role is of minor importance.

### 2.2. DFT mechanistic studies

The catalytic role of discrete molecules of $H_2O$ in the neutral and ionic forms of taxifolin and phloroglucinol was investigated using various DFT levels of theory (B3LYP, PBE0, APFD, M06-2X, ωB97X-D, B3LYP/GD3BJ, PBE0/GD3BJ, and CAM-B3LYP/GD3BJ) and the 6-31+G(d) basis set.[30–32] Basis sets of this size give better results than large basis sets due to the cancellation of errors.[33] At the highest level of theory and basis set, it is evident that all protons move simultaneously.

 

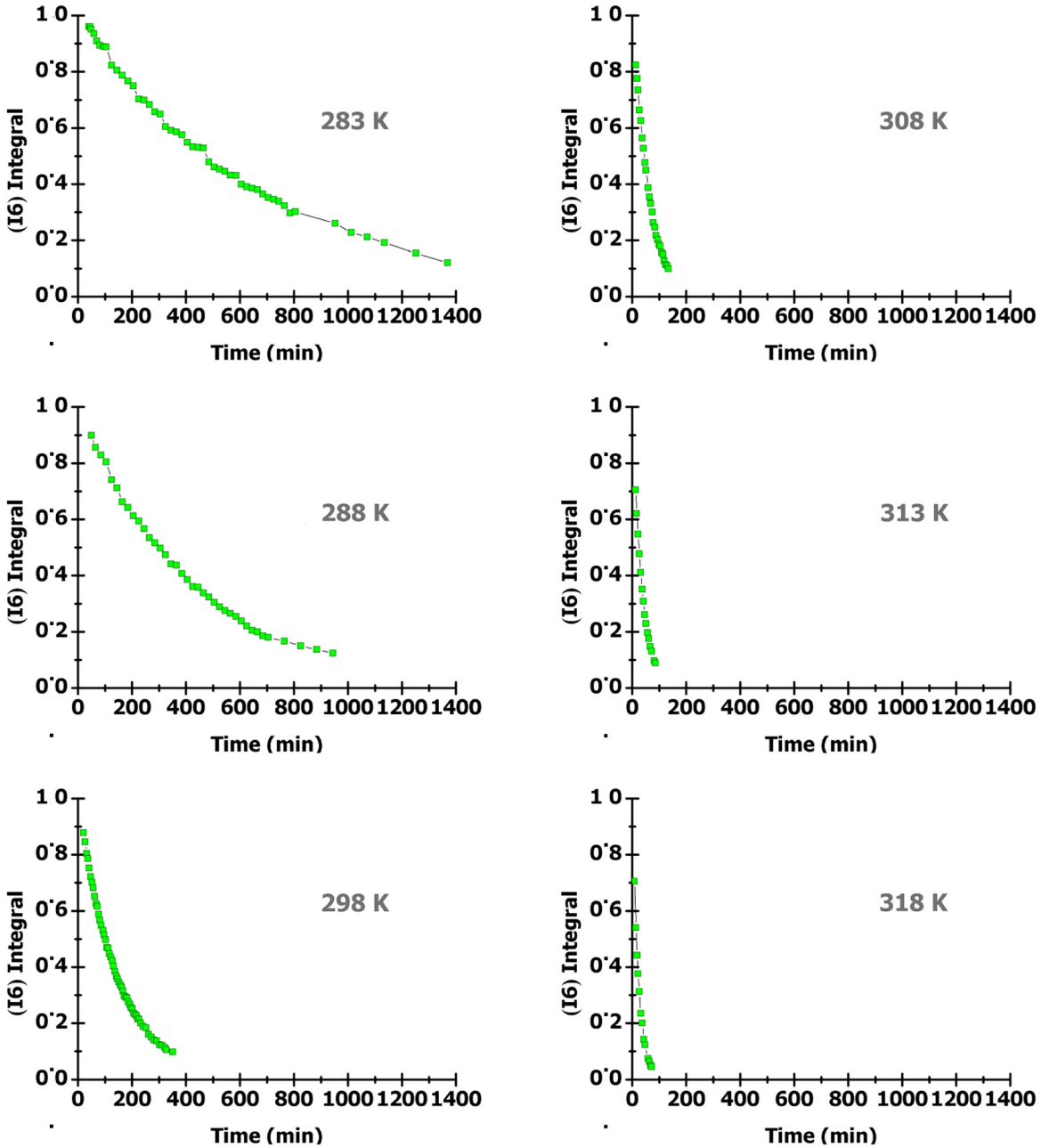


Fig. 4 H-6 H/D exchange kinetic curves of taxifolin (2.5 mM) in $D_2O$, phosphate buffer (25 mM), and pD = 9.60 at various temperatures.

**2.2.1. The neutral form of phloroglucinol and taxifolin-effects of two-to-four molecules $H_2O$.** Various mechanistic pathways of the neutral form of phloroglucinol were examined with two to four molecules of $H_2O$ in various "in–in", and "in–out" orientations of the phenol OH groups (Table 2 and Table S1, ESI†). The computational data with two molecules of $H_2O$ in the transition state resulted in $\Delta G^{\ddagger}_{comp}$ values in the range of 23.15 to 27.11 kcal $mol^{-1}$ which deviate from the experimental value of 20.96 kcal $mol^{-1}$ (Table 2 and Table S1, ESI†). The only exceptions are the computational data of the APFD/6-31+G(d) method with $\Delta G^{\ddagger}_{comp} =$ 20.59 kcal $mol^{-1}$, which is in excellent agreement with the experimental value (Fig. 7). Of particular interest is the lengthening of the C(1)O–H bond from 0.983 Å in the ground state to 1.540 Å in the transition state and the shortening of the HO–H···C(2)H distance from 2.425 Å in the ground state to 1.523 Å in the transition state. The computational data demonstrate that the enthalpic activation energy $\left(\Delta H^{\ddagger}_{comp} = 17.21 \text{ to } 22.65 \text{ kcal mol}^{-1}\right)$ is significantly larger than the entropic activation energy $\left(-T\Delta S^{\ddagger}_{comp} = 2.10 \text{ to } 5.24 \text{ kcal mol}^{-1}\right)$ which is in excellent agreement with the experimental data ($\Delta H^{\ddagger}_{exp} = 17.46$ kcal $mol^{-1}$ and $-T\Delta S^{\ddagger}_{exp} = 3.50$ kcal $mol^{-1}$). The minor role of the $-T\Delta S^{\ddagger}_{exp}$ term could be attributed to

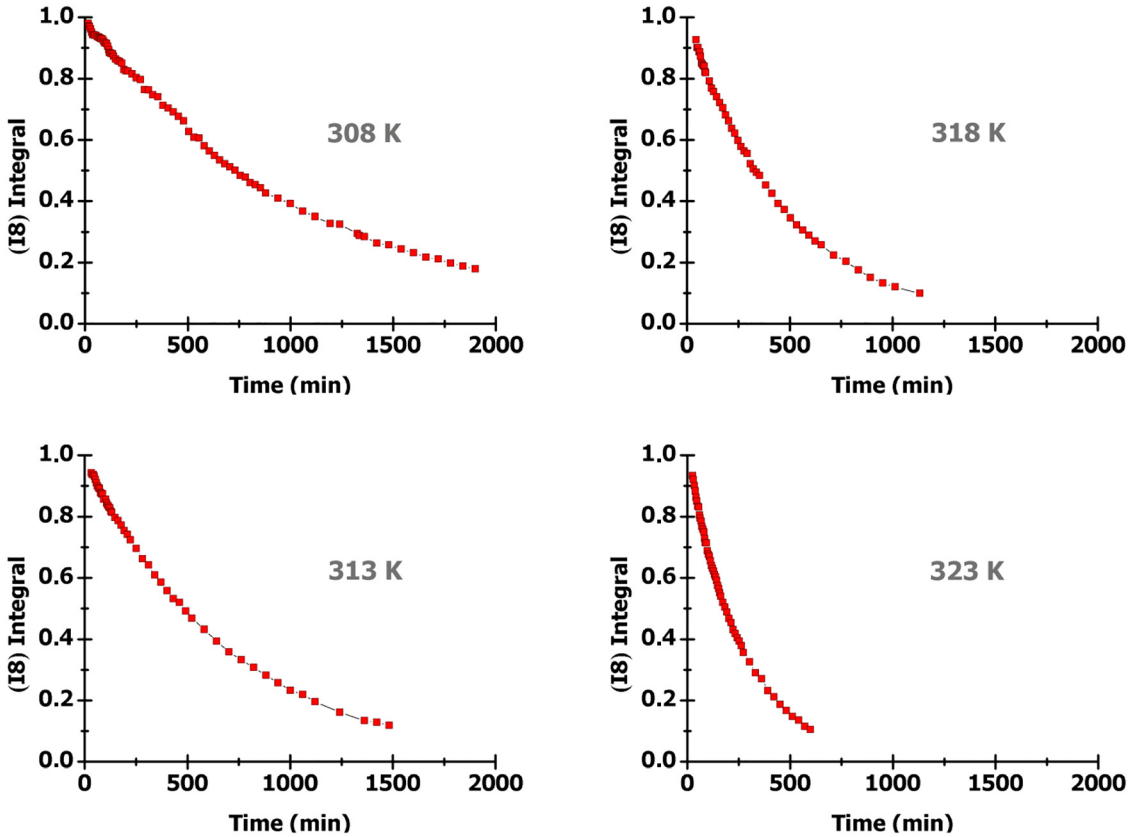


Fig. 5 H-8 H/D exchange kinetic curves of taxifolin (2.5 mM) in $D_2O$, phosphate buffer (25 mM), and pD = 9.60 at various temperatures.

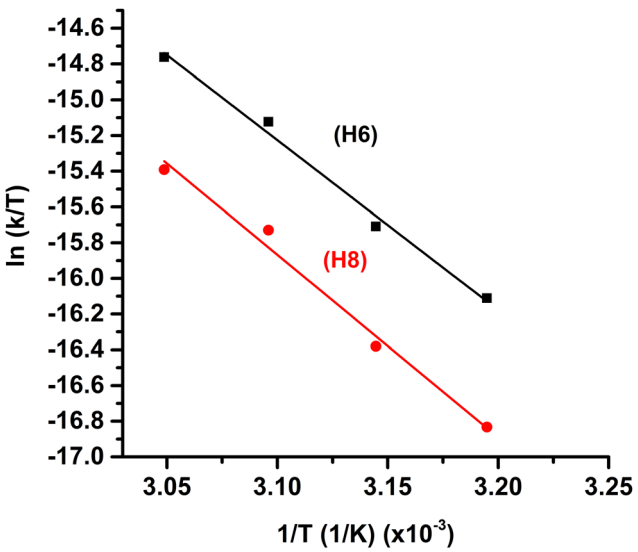


Fig. 6 Eyring plots of the H-6 ($R^2$ = 0.988) and H-8 ($R^2$ = 0.982) of taxifolin (2.5 mM) in $D_2O$, phosphate buffer (25 mM), and pD = 6.00.

the relatively small increase of entropy in the transition state, which indicates a dissociative mechanism of the loosely bound activated complex.

In the case of the complex of phloroglucinol with three molecules of $H_2O$, four reactions mechanisms were examined with the OH groups in the "in–out" and "in–in" configuration (Fig. 8). In the "in–out" and "in–out A" configurations (with slightly different hydrogen bond network of the molecules of $H_2O$, Fig. 8A) two $\Delta G^{\ddagger}_{comp}$ values of 26.28 and 23.03 kcal mol$^{-1}$ were obtained with relative Boltzmann populations of 10.9% and 0.04%, respectively, which deviate significantly from the experimental value $\left(\Delta G^{\ddagger}_{exp} = 20.96 \text{ kcal mol}^{-1}\right)$. In contrast, in the "in–in" and "in–in A" configurations, the resulting $\Delta G^{\ddagger}_{comp}$ values of 20.13 and 19.75 kcal mol$^{-1}$ with relative Boltzmann populations of 58.5% and 30.5% are in excellent agreement with the experimental value. In the transition state of the "in–in" and "in–in A" configurations, the oxygen atom of the central molecule of $H_2O$ forms a closer contact with the C(2)–H bond of 1.451 Å, contrary to 1.600 Å in the "in–out" and in the "in–out A" configurations (Fig. 8). This demonstrates that the relative configuration of the phenol OH groups could have a significant effect on the $\Delta G^{\ddagger}$ values and, thus, on the reaction mechanisms. Again, the $\Delta G^{\ddagger}_{comp}$ term is significantly larger than the $-T\Delta S^{\ddagger}_{comp}$ term, which is in excellent agreement with the experimental data.

In the case of the complex of phloroglucinol with four molecules of $H_2O$, three reaction mechanisms were examined with the OH groups in the "in–out", "in–in". and "in–in A" configuration (Fig. S1, ESI†). In the "in–in A" and "in–in" configurations, the $\Delta G^{\ddagger}_{comp}$ = 20.75 and 20.39 kcal mol$^{-1}$

 

Table 1 Activation enthalpy $\left(\Delta H^{\ddagger}_{exp}\right)$, activation entropy $\left(\Delta S^{\ddagger}_{exp}\right)$ and Gibbs activation energy $\left(\Delta G^{\ddagger}_{exp}\right)$ for H/D exchange reactions of the H-8 and H-6 protons of taxifolin (2.5 mM) at various pD values and phosphate buffer concentrations

| | | | H-8 | | | H-6 | | |
|---|---|---|---|---|---|---|---|---|
| Compound | Buffer concentration | pD | $\Delta H^{\ddagger}_{exp}$ (kcal mol$^{-1}$) | $-T\Delta S^{\ddagger}_{exp}$ (kcal mol$^{-1}$) | $\Delta G^{\ddagger}_{exp}$ (kcal mol$^{-1}$) | $\Delta H^{\ddagger}_{exp}$ (kcal mol$^{-1}$) | $-T\Delta S^{\ddagger}_{exp}$ (kcal mol$^{-1}$) | $\Delta G^{\ddagger}_{exp}$ (kcal mol$^{-1}$) |
| Taxifolin | 25 mM | 6.0 | 20.31 ± 1.57 | 4.70 ± 0.79 | 25.01 | 18.91 ± 1.18 | 5.62 ± 0.59 | 24.53 |
| | 25 mM | 7.6 | 18.79 ± 1.59 | 5.80 ± 0.80 | 24.59 | 14.01 ± 1.47 | 9.17 ± 0.82 | 23.18 |
| | 50 mM | 7.6 | 19.34 ± 1.18 | 5.05 ± 0.65 | 24.39 | 20.63 ± 1.26 | 2.24 ± 0.49 | 22.87 |
| | 25 mM | 9.6 | 18.43 ± 1.79 | 6.24 ± 0.72 | 24.67 | 16.67 ± 0.55 | 6.15 ± 0.55 | 22.81 |
| | 50 mM | 9.6 | 19.62 ± 0.77 | 4.07 ± 0.65 | 23.69 | 16.96 ± 0.54 | 5.51 ± 0.58 | 22.46 |
| | 1 M | 9.6 | 15.96 ± 1.22 | 7.98 ± 0.78 | 23.94 | 11.76 ± 0.75 | 10.38 ± 0.98 | 22.14 |
| Phloroglucinol[a] | | | H-2,4,6 | | | | | |
| | 25 mM | 6.9 | 17.46 ± 0.30 | 3.50 ± 0.09 | 20.96 | | | |
| | 25 mM | 7.9 | 16.05 ± 0.78 | 3.69 ± 0.26 | 19.74 | | | |
| | 25 mM | 8.9 | 16.55 ± 1.15 | 2.86 ± 0.29 | 19.41 | | | |

[a] Ref. 17.

Table 2 Selected computed Gibbs activation energy $\left(\Delta G^{\ddagger}_{comp}\right)$ (kcal mol$^{-1}$) for neutral and ionic forms of phloroglucinol and taxifolin for various molecular $H_2O$ solvation species and computational methods (for complete set of data see Tables S1–S3, ESI). In parenthesis are the Boltzmann populations

| | | +3$H_2O$ | | |
|---|---|---|---|---|
| Neutral phloroglucinol | +2$H_2O$ | "in–out" | "in–in" "in–in A" | Exp. |
| APFD/6-31+G(d) | 20.59 | 26.28 (10.94%) | 20.13 (58.52%)<br>19.75 (30.51%) | 20.96 |
| B3LYP/6-31+G(d)/GD3BJ | 23.15 | 27.52 (14.19%) | 21.66 (46.80%)<br>21.54 (38.19%) | |
| PBE0/6-31+G(d)/GD3BJ | 23.16 | 27.76 (9.65%) | 21.65 (51.47%)<br>21.48 (38.75%) | |
| ωB97XD/6-31+G(d) | 26.19 | 30.86 (17.12%) | 25.08 (52.04%)<br>24.76 (30.36%) | |
| CAM-B3LYP/6-31+G(d)/GD3BJ | 24.68 | 29.71 (16.10%) | 23.99 (46.39%)<br>23.62 (37.37%) | |

| | +2$H_2O$ | | +3$H_2O$ | | Exp. | |
|---|---|---|---|---|---|---|
| Neutral taxifolin | C-6 | C-8 | C-6 | C-8 | C-6 | C-8 |
| APFD/6-31+G(d) | 20.79 | 20.77 | 22.98 | 23.55 | 24.53 | 25.01 |
| B3LYP/6-31+G(d)/GD3BJ | 20.81 | 21.93 | 25.63 | 24.72 | | |
| PBE0/6-31+G(d)/GD3BJ | 20.80 | 21.28 | 25.18 | 24.67 | | |
| ωB97XD/6-31+G(d) | 25.08 | 24.19 | 27.38 | 27.37 | | |
| CAM-B3LYP/6-31+G(d) | 24.78 | 25.67 | 29.12 | 28.81 | | |
| CAM-B3LYP/6-31+G(d)/GD3BJ | 22.69 | 23.59 | 27.26/27.05 | 27.66 | | |

| | +2$H_2O$ | | | | |
|---|---|---|---|---|---|
| Ionic phloroglucinol | on OH | C═O (A) | C═O (B) | +3$H_2O$ | Exp. |
| APFD/6-31+G(d) | 11.83 | 19.15 | [a] | 11.26 | 19.74 |
| B3LYP/6-31+G(d)/GD3BJ | 13.01 (0.26%) | 19.91 (33.85%) | 19.86 (65.89%) | 11.63 | |
| PBE0/6-31+G(d)/GD3BJ | 13.05 | 19.71 | [a] | 11.48 | |
| ωB97XD/6-31+G(d) | 15.21 (0.37%) | 22.16 (41.71%) | 21.37 (57.92%) | 14.07 | |
| CAM-B3LYP/6-31+G(d) | 14.39 (0.32%) | 21.69 (60.95%) | 20.58 (38.73%) | 13.36 | |
| CAM-B3LYP/6-31+G(d)/GD3BJ | 14.08 (0.30%) | 21.32 (39.49%) | 20.47 (60.20%) | 12.95 | |

| | | +3$H_2O$ | | Exp. | |
|---|---|---|---|---|---|
| Ionic taxifolin | +2$H_2O$ | C-6 | C-8 | C-6 | C-8 |
| B3LYP/6-31+G(d)/GD3BJ | [a] | 23.83 | 24.27 | 23.18 | 24.59 |
| PBE0/6-31+G(d)/GD3BJ | [a] | 24.76 | 26.00 | | |
| ωB97XD/6-31+G(d) | [a] | 24.51 | 26.18 | | |
| CAM-B3LYP-D/6-31+G(d) | [a] | 23.44 | 22.80 | | |

[a] A transition state could not be determined.

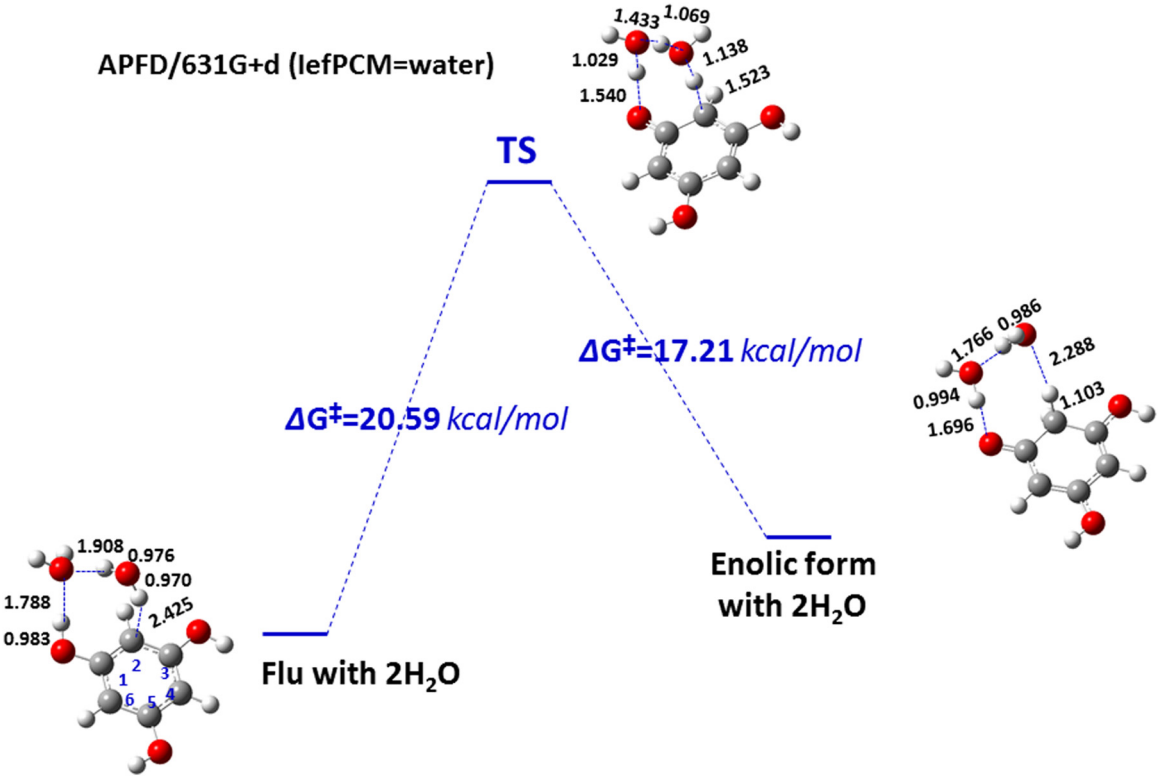


Fig. 7 The mechanistic pathway of the aromatic hydrogen exchange process of the complex of the neutral phloroglucinol (Flu) with two molecules of $H_2O$ with the APFD/6-31+G(d) method.

(at the B3LYP/6-31+G(d)/GD3BJ level) with relative Boltzmann populations of 77.9% and 22.6%, respectively, are in excellent agreement with the experimental value. The $\Delta G^{\ddagger}_{comp}$ value of 21.97 kcal $mol^{-1}$ with a Boltzmann population of 0.02% deviates from the experimental value. It can be concluded that: (i) the increase in the number of catalytically important molecules of $H_2O$ from three to four does not improve significantly the agreement of computational results with the experimental data. (ii) In all complexes with two to four molecules of $H_2O$, the relatively small increase of entropy in the transition state indicates a dissociative mechanism of the loosely bound activated complex.

From the mechanistic point of view, the case of taxifolin is simpler than that of phloroglucinol since the C-6 and C-8 positions were examined with a single orientation of the OH(5) group due to the formation of a strong intramolecular hydrogen bond with the C(4)O group,[34–37] which persists in organic and aqueous solutions.[34] This significantly reduces the number of the available mechanistic pathways in the transition state. The computational Gibbs activation energies, with two molecules of $H_2O$ in the transition state, at the ωB97XD/6-31+G(d) level $\left(\Delta G^{\ddagger}_{comp}(\text{C-6}) = 25.08 \text{ kcal mol}^{-1} \text{ and } \Delta G^{\ddagger}_{comp}(\text{C-8}) = 24.19 \text{ kcal mol}^{-1}\right)$ and at the CAM-B3LYP/6-31+G(d) level $(\Delta G^{\ddagger}_{comp}(\text{C-6}) = 24.78 \text{ kcal mol}^{-1}$ and $\Delta G^{\ddagger}_{comp}(\text{C-8}) = 25.67 \text{ kcal mol}^{-1})$ are in excellent agreement with $\Delta G^{\ddagger}_{exp}(\text{C-6}) = 24.53 \text{ kcal mol}^{-1}$ and $(\Delta G^{\ddagger}_{exp}(\text{C-8}) = 25.67 \text{ kcal mol}^{-1}$ (Table 2 and Table S2, ESI†)). It is of interest that at the CAM-B3LYP/6-31+G(d) level, the small increase in $\Delta G^{\ddagger}_{exp}$ (C-8) relative to $\Delta G^{\ddagger}_{comp}$ (C-6) is reproduced correctly. The other functionals result in smaller $\Delta G^{\ddagger}_{comp}$ values, such as with the APDF/6-31+G(d) method (Fig. 9A). The use of three molecules of $H_2O$ in the transition state results in larger $\Delta G^{\ddagger}_{comp}$ values than those obtained with two molecules of $H_2O$ (Table 2, Table S2 (ESI†) and Fig. 9B). At the B3LYP/6-31+G(d)/GD3BJ and PBE0/6-31+G(d)/DG3BJ levels, the $\Delta G^{\ddagger}_{comp}$ values are in very good agreement with the experimental data, contrary to the case of CAM-B3LYP/6-31+G(d) and CAM-B3LYP/6-31+G(d)/GD3BJ. In all cases, the $\Delta H^{\ddagger}_{comp}$ values are significantly larger than the $-T\Delta S^{\ddagger}_{comp}$ values, in very good agreement with the experimental data. Inclusion of four molecules of water in the transition state does not improve the agreement between $\Delta G^{\ddagger}_{comp}$ and $\Delta G^{\ddagger}_{exp}$ for both the C-6 and C-8 hydrogens (Table S2, ESI†). Interestingly, the entropic term $-T\Delta S^{\ddagger}_{comp}$ reduces significantly and for some functionals, it becomes negative which is contrary to the experimental data (Table 1).

**2.2.2. The ionic form of phloroglucinol and taxifolin-effects of two-to-four molecules of water.** While for the neutral molecules, the location of the transition state was obtained by guessing the most probable structure, and the anionic form was far more demanding. Thus, we thoroughly scanned the potential energy surface (PES), defining the protons participating in the transfer as reaction coordinates. Upon inspection,

 

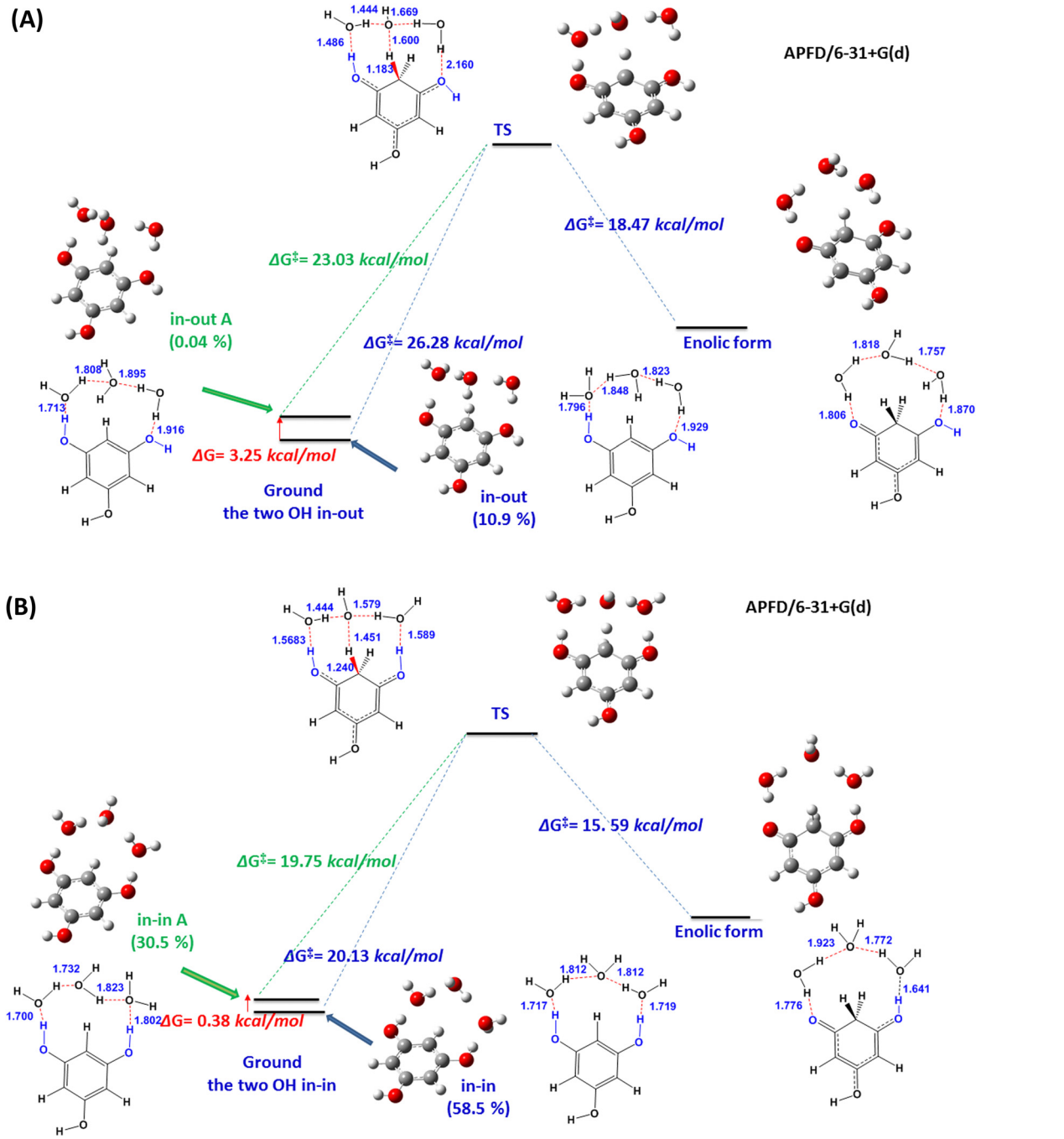


Fig. 8 The mechanistic pathways of the aromatic hydrogen exchange process of the complex of neutral phloroglucinol with three molecules of $H_2O$ and the two phenol –OH groups in the "in–out" (A) and "in–in" (B) configurations at the APFD/6-31+G(d) level. In parenthesis are the Boltzmann populations (Table 2 and Table S1, ESI†).

saddle points were located and subsequently tested successfully as possible transition states.

In the phloroglucinol anion, as in the case of the neutral form, several possible mechanistic pathways were investigated with two to four molecules of $H_2O$ in the transition state (Table 2 and Table S3, ESI†). For the complex of the phloroglucinol anion with two molecules of $H_2O$, the reaction mechanism with one bound molecule of $H_2O$ on the OH group resulted in very low Boltzmann population and $\Delta G^{\ddagger}_{comp}$ values (11.83 to 17.83 kcal $mol^{-1}$) which strongly deviate from the experimental data $\left(\Delta G^{\ddagger}_{exp} = 19.74 \text{ kcal mol}^{-1}\right)$. In contrast, the reaction mechanisms (A and B, Fig. 10) with one bound molecule of $H_2O$ on the C=O moiety resulted in high Boltzmann populations and very good agreement with the experimental data, especially at the B3LYP/6-31+G(d)/GD3BG level

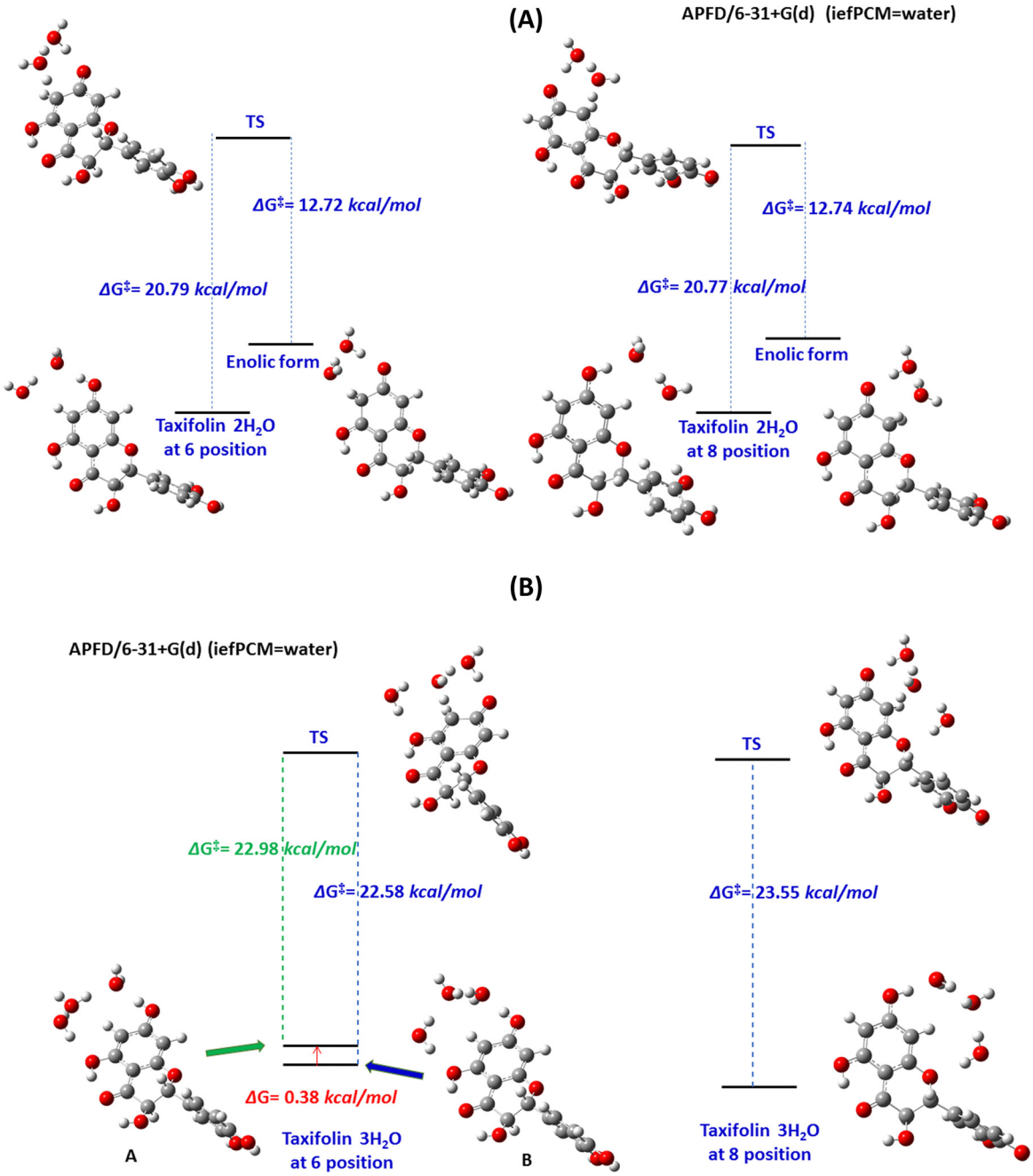


Fig. 9 The mechanistic pathway of the aromatic C(8)–H and C(6)–H hydrogen exchange process of the complex of the neutral taxifolin with two (A) and three (B) molecules of $H_2O$ at the APFD/6-31+G(d) level.

$\left(\Delta G^{\ddagger}_{comp} = 19.86 \text{ and } 19.65 \text{ kcal mol}^{-1}\right)$ (Fig. 10b, c, Table 2 and Table S2, ESI†).

The computational data with three molecules of $H_2O$ in the transition state $\left(\Delta G^{\ddagger}_{comp} = 11.26 \text{ to } 16.47 \text{ kcal mol}^{-1}\right)$ strongly deviate from the experimental data (Table S3, ESI†). Similarly, the computational data with four molecules of $H_2O$ strongly deviate from the experimental data $\left(\Delta G^{\ddagger}_{comp} = 12.95 \text{ to } 17.71 \text{ kcal mol}^{-1}\right)$. In both cases, the enthalpic activation energy $\left(\Delta H^{\ddagger}_{comp}\right)$ is strongly underestimated (Table S3, ESI†).

For the taxifolin anion, the ring C (Fig. 1) was substituted by a methyl group to facilitate computations. In the case of the complex with two molecules of $H_2O$, a transition state could not be determined using a variety of functionals and basis sets (Table 2 and Table S4, ESI†). In contrast, with three molecules of $H_2O$ in the transition state, the majority of the functionals and basis set used resulted in $\Delta G^{\ddagger}_{comp}$(C-6) = 23.44 to 24.76 kcal mol$^{-1}$ and $\Delta G^{\ddagger}_{comp}$(C-8) = 22.80 to 26.18 kcal mol$^{-1}$, in excellent agreement with the experimental values $\Delta G^{\ddagger}_{exp}$(C-6) = 23.18 kcal mol$^{-1}$ and $\Delta G^{\ddagger}_{exp}$(C-8) = 24.59 kcal mol$^{-1}$ (Table 2 and Table S4, ESI†).

 

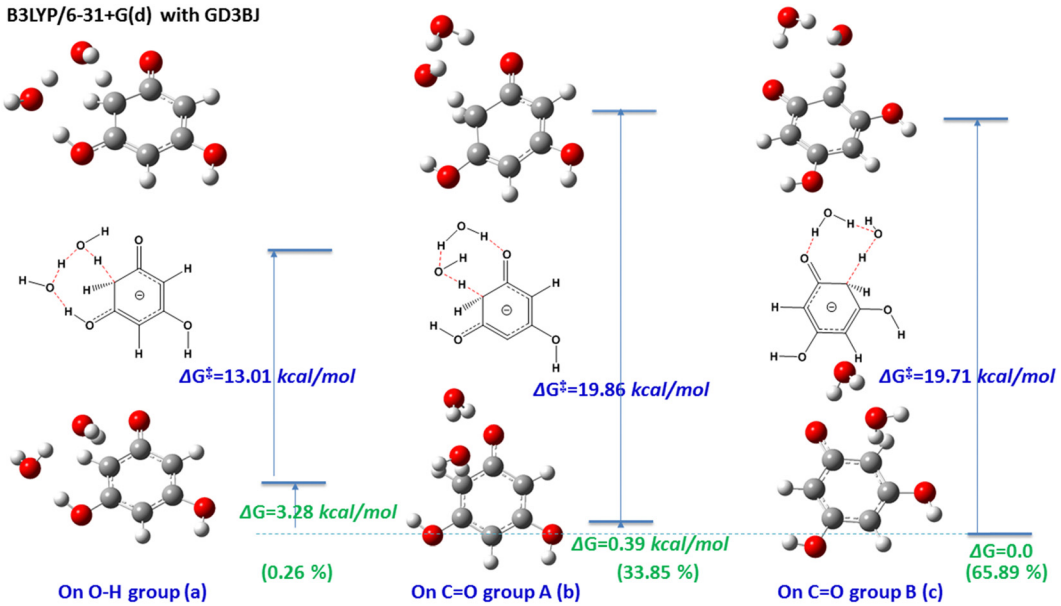


Fig. 10 Three possible mechanistic pathways of the aromatic hydrogen exchange process of the phloroglucinol anion with two molecules of $H_2O$: one molecule of $H_2O$ on the phenol –OH group (a), and one molecule of $H_2O$ on the C═O bond (b) and (c), at the B3LYP/6-31+G(d)/D3BJ level.

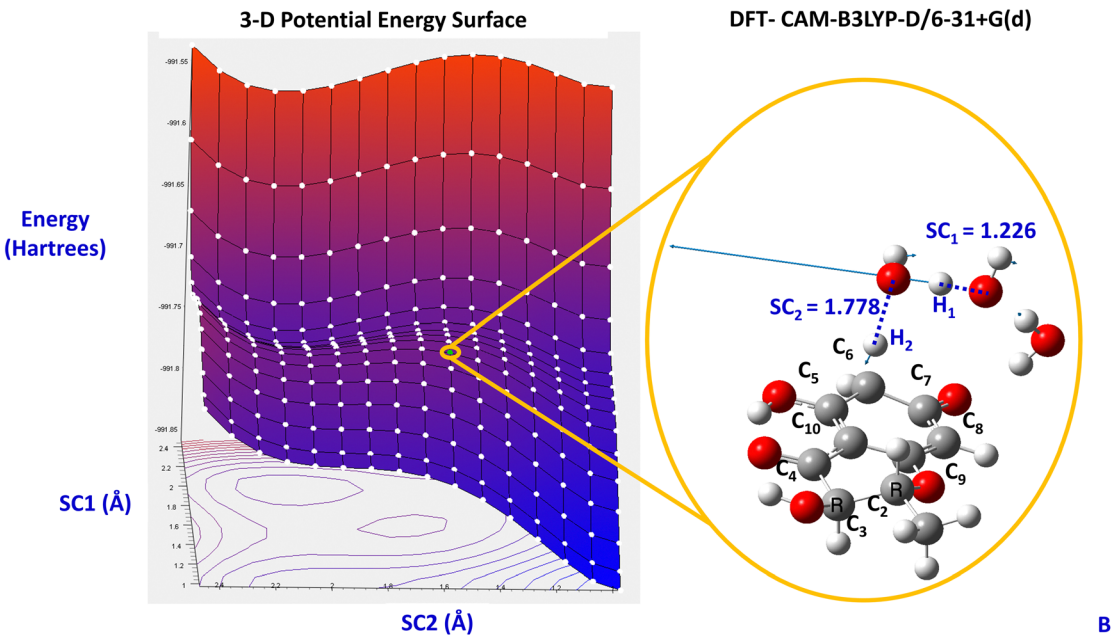


Fig. 11 Potential energy scan of the ionic form of taxifolin with three catalytically important molecules of $H_2O$.

Fig. 11 presents the potential energy scan (PES) of the ionic form of taxifolin with three catalytically important molecules of $H_2O$. The PES indicated various values of saddle points of the electronic energy function of the two scan coordinates (SC1 and SC2 shown in Fig. 11B) that represent the systematic proton translocation [Eel = f(SC1, SC2)]. From the systematic optimization of these saddle points, we located the transition state described in Fig. 11B. The adopted approach underlines the importance of the systematic search of transition states which are difficult to locate.

## 3. Computational details

Calculations of the neutral and ionic forms of phloroglucinol and taxifolin were performed with a variety of DFT methods (B3LYP, PBE0 (PBE1PBE), APFD, M06-2X and ωB97XD) using

the 6-31+G(d) basis set as well as with the B3LYP/6-31+G(d)/GD3BJ and PBE1PBE/6-31+G(d)/GD3BJ level hybrid functionals as implemented in the Gaussian 09W Package.[38] Additional computations were performed at the CAM-B3LYP-D/6-31+G(d) level. In all cases, the polarized continuum model IEF-PCM (integral equation formalism-polarizable continuum model) was used in $H_2O$. In order to investigate the transition state, as well as the structure of the products, calculations were carried out at the same level of theory using the gas phase and IEF-PCM model. The computed geometries were verified as minima by frequency calculations at the same level of theory (no imaginary frequencies).

## 4. Conclusions

In summary, variable temperature and pD $^1$H NMR studies of the activation enthalpy $\left(\Delta H^{\ddagger}_{\text{exp}}\right)$, entropy $\left(-T\Delta S^{\ddagger}_{\text{exp}}\right)$ and Gibbs free energy $\left(\Delta G^{\ddagger}_{\text{exp}}\right)$ of H/D exchange reactions of the H-6 and H-8 protons belonging to ring A of the natural product taxifolin are reported. The $\Delta G^{\ddagger}_{\text{exp}}$ values are in the range of $\sim$25 to 23 kcal mol$^{-1}$ for pD values of 6.1 to 9.6 and practically independent of the buffer concentration. Differences in $\Delta G^{\ddagger}_{\text{exp}}$ values of neutral and anionic taxifolin and phloroglucinol were found to be very small ($\leq$1.5 kcal mol$^{-1}$). Excellent agreement between $\Delta G^{\ddagger}_{\text{exp}}$ and DFT calculated Gibbs free activation energies, $\Delta G^{\ddagger}_{\text{comp}}$, was obtained, especially at the APFD/6-31+G(d) and B3LYP/6-31+G(d)/GD3BJ levels, with the use of three molecules of $H_2O$ in the transition state for the neutral state of phloroglucinol (with the ''in–in'' configuration of the phenol OH groups) and taxifolin. In the ionic form of phloroglucinol, the mechanistic pathway with two molecules of $H_2O$ in the transition state (one of which involves the C=O moiety), showed very good agreement with the experimental data. For the anionic form of taxifolin, the mechanistic pathway with three molecules of $H_2O$ in the transition state showed excellent agreement with the experimental $\Delta G^{\ddagger}_{\text{exp}}$ values. The enthalpic term $\Delta H^{\ddagger}_{\text{comp}}$ is considerably larger than the entropic $-T\Delta S^{\ddagger}_{\text{comp}}$ term, which is in excellent agreement with the experimental data. This indicates a dissociative mechanism of the loosely bound activated complex. The present results are important for the following reasons:

(i) The catalytic role of two and/or three molecules of $H_2O$ through keto–enol tautomerization, which is a many body cooperative effect of hydrogen-bonded $H_2O$ molecules in proton translocation, brought into question the generally accepted acid/base catalyzed H/D exchange mechanism emphasized in undergraduate chemistry textbooks.

(ii) Water catalysis plays a significant role at neutral pH values and near ambient temperatures thus, by definition, is a green approach by avoiding strong acid and basic conditions.

## Author contributions

Photini Chalkidou: performed the NMR experiments. Themistoklis Venianakis: performed the NMR experiments. George Papamokos: performed DFT computations, analyzed computational data and prepared the manuscript. Michael Siskos: performed DFT computations, conceived and designed the project, analyzed the experimental and computational data and prepared the manuscript. Ioannis P. Gerothanassis: conceived and designed the project, analyzed the experimental and computational data and prepared the manuscript.

## Data availability

The data supporting this article have been included as part of the ESI.†

## Conflicts of interest

There are no conflicts to declare.

## Acknowledgements

The use of the NMR Core Facility of the University of Ioannina is gratefully acknowledged. This work was supported by Greek Community Support Framework III, Regional Operational, MIS 91629.

## Notes and references

1 M. F. Ruiz-Lopez, J. S. Francisco, M. T. C. Martins-Costa and J. M. Anglada, *Nat. Rev. Chem.*, 2020, **4**, 459–475.
2 T. Kitanosono and S. Kobayashi, *Chem. Eur. J.*, 2020, **26**, 9408–9429.
3 L. Lin, Y. Ge, H. Zhang, M. Wang, D. Xiao and D. Ma, *J. Am. Chem. Soc. Au*, 2021, **1**, 1834–1848.
4 M. Cortes-Clerget, J. Yu, J. R. A. Kincaid, P. Walde, F. Gallou and B. H. Lipshutz, *Chem. Sci.*, 2021, **12**, 4237–4266.
5 H. Gröger, F. Gallou and B. H. Lipshutz, *Chem. Rev.*, 2023, **123**, 5262–5296.
6 G. Li, Y. Dai, Y. Yang and D. E. Resasco, *Chem. Catal.*, 2021, **1**, 959–965.
7 P. M. Yavorsky and E. Gorin, *J. Am. Chem. Soc.*, 1962, **84**, 1071–1072.
8 P. McGeady and R. A. Croteau, *J. Chem. Soc., Chem. Commun.*, 1993, **9**, 774–776.
9 P. S. Kiuru and K. Wähälä, *Steroid*, 2006, **71**, 54–60.
10 J. Atzrodt, V. Derdau, T. Fey and J. Zimmermann, *Angew. Chem., Int. Ed.*, 2007, **46**, 7744–7765.
11 M. Jordheim, T. Fossen, J. Songstad and O. M. Andersen, *J. Agric. Food Chem.*, 2007, **55**, 8261–8268.
12 A. J. Kresge and Y. Chiang, *J. Am. Chem. Soc.*, 1961, **83**, 2877–2885.
13 E. S. Hand and R. M. Horowitz, *J. Am. Chem. Soc.*, 1964, **86**, 2084–2085.
14 P. Ryberg and O. Matsson, *J. Org. Chem.*, 2002, **67**, 811–814.
15 S. H. M. Mehr, K. Fukuyama, S. Bishop, F. Lelj and M. J. MacLachlan, *J. Org. Chem.*, 2015, **80**, 5144–5150.

 

16 F. Bonaldo, F. Mattivi, D. Catorci, P. Arapitsas and G. Guella, *Molecules*, 2021, **26**, 3544.
17 A. Fayaz, M. G. Siskos, P. C. Varras, M. I. Choudhary, A. T. Wahab and I. P. Gerothanassis, *Phys. Chem. Chem. Phys.*, 2020, **22**, 17401–17411.
18 R. Breslow, *Acc. Chem. Res.*, 1991, **24**, 159–164.
19 S. Narayan, J. Muldoon, M. G. Finn, V. V. Fokin, H. C. Kolb and K. B. Sharpless, *Angew. Chem., Int. Ed.*, 2005, **44**, 3275–3279.
20 U. M. Lindström, *Chem. Rev.*, 2002, **102**, 2751–2772.
21 A. Chanda and V. V. Fokin, *Chem. Rev.*, 2009, **109**, 725–748.
22 Y. Jung and R. A. Marcus, *J. Am. Chem. Soc.*, 2007, **129**, 5492–5502.
23 T. G. Kim, Y. Kim and D.-J. Jang, *J. Phys. Chem. A*, 2001, **105**, 4328–4332.
24 S. Otto and J. B. Engberts, *Org. Biomol. Chem.*, 2003, **1**, 2809–2820.
25 N. A. Isley, R. T. Linstadt, S. M. Kelly, F. Gallou and B. H. Lipshutz, *Org. Lett.*, 2015, **17**, 4734–4737.
26 T. Kitanosono, K. Masuda, P. Xu and S. Kobayashi, *Chem. Rev.*, 2018, **118**, 679–746.
27 G. Alagona, C. Ghio and P. I. Nagy, *Phys. Chem. Chem. Phys.*, 2010, **12**, 10173–10188.
28 J. M. Saa and A. Frontera, *Chem. Phys. Chem.*, 2020, **21**, 313–320.
29 J. M. Herrero-Martínez, M. Sanmartin, M. Rosés, E. Bosch and C. Ràfols, *Electrophoresis*, 2005, **26**, 1886–1895.
30 S. Grimme, S. Ehrlish and L. Goerigk, *J. Comput. Chem.*, 2011, **32**, 1456–1465.
31 Y. Zhao and D. G. Truhlar, *J. Phys. Chem.*, 2006, **110**, 5121–5129.
32 J.-D. Chai and M. Head-Gordon, *Phys. Chem. Chem. Phys.*, 2008, **10**, 6615–6620.
33 X. Xuefei, I. M. Alecu and G. Donald, *J. Chem. Theory Comput.*, 2011, **7**(6), 1667–1676.
34 V. Exarchou, A. N. Troganis, I. P. Gerothanassis, M. Tsimidou and D. Boskou, *Tetrahedron*, 2002, **58**, 7423–7429.
35 P. Charisiadis, V. Exarchou, A. N. Troganis and I. P. Gerothanassis, *Chem. Commun.*, 2010, **46**, 3589–3591.
36 S. H. Mari, P. C. Varras, A.-T. Wahab, I. M. Choudhary, M. G. Siskos and I. P. Gerothanassis, *Molecules*, 2019, **24**, 2290.
37 P. Charisiadis, T. Venianakis, C. D. Papaemmanouil, A. Primikyri, A. G. Tzakos, M. G. Siskos and I. P. Gerothanassis, *Magn. Reson. Chem.*, 2025, **63**, 170–179.
38 M. J. Frisch, G. W. Trucks, H. B. Schlegel, G. E. Scuseria, M. A. Robb, J. R. Cheeseman, G. Scalmani, V. Barone, B. Mennucci, G. A. Petersson, H. Nakatsuji, M. Caricato, X. Li, H. P. Hratchian, A. F. Izmaylov, J. Bloino, G. Zheng, J. L. Sonnenberg, M. Hada, M. Ehara, K. Toyota, R. Fukuda, J. Hasegawa, M. Ishida, T. Nakajima, Y. Honda, O. Kitao, H. Nakai, T. Vreven, J. A. MontgomeryJr, J. E. Peralta, F. Ogliaro, M. Bearpark, J. J. Heyd, E. Brothers, K. N. Kudin, V. N. Staroverov, T. Keith, R. Kobayashi, J. Normand, K. Raghavachari, A. Rendell, J. C. Burant, S. S. Iyengar, J. Tomasi, M. Cossi, N. Rega, J. M. Millam, M. Klene, J. E. Knox, J. B. Cross, B. Bakken, C. Adamo, J. Jaramillo, R. Gomperts, R. E. Stratmann, O. Yazyev, A. J. Austin, R. Cammi, C. Pomelli, J. W. Ochterski, R. L. Martin, K. Morokuma, V. G. Zakrzewski, G. A. Voth, P. Salvador, J. J. Dannenberg, S. Dapprich, A. D. Daniels, O. Farkas, J. B. Foresman, J. V. Ortiz, J. Cioslowski and D. J. Fox, *D. J. Gaussian 09, revision B.01*, Gaussian, Inc., Wallingford, CT, 2010.